

Quantum rotor theory of spinor condensates in tight traps

Ryan Barnett, Hoi-Yin Hui, Chien-Hung Lin, Jay D. Sau, and S. Das Sarma

Joint Quantum Institute and Condensed Matter Theory Center, Department of Physics, University of Maryland, College Park, Maryland 20742-4111, USA

(Received 1 December 2010; published 22 February 2011)

In this work, we theoretically construct exact mappings of many-particle bosonic systems onto quantum rotor models. In particular, we analyze the rotor representation of spinor Bose-Einstein condensates. In a previous work [R. Barnett *et al.*, *Phys. Rev. A* **82**, 031602(R) (2010)] it was shown that there is an exact mapping of a spin-one condensate of fixed particle number with quadratic Zeeman interaction onto a quantum rotor model. Since the rotor model has an unbounded spectrum from above, it has many more eigenstates than the original bosonic model. Here we show that for each subset of states with fixed spin F_z , the physical rotor eigenstates are always those with the lowest energy. We classify three distinct physical limits of the rotor model: the Rabi, Josephson, and Fock regimes. The last regime corresponds to a fragmented condensate and is thus not captured by the Bogoliubov theory. We next consider the semiclassical limit of the rotor problem and make connections with the quantum wave functions through the use of the Husimi distribution function. Finally, we describe how to extend the analysis to higher-spin systems and derive a rotor model for the spin-two condensate. Theoretical details of the rotor mapping are also provided here.

DOI: [10.1103/PhysRevA.83.023613](https://doi.org/10.1103/PhysRevA.83.023613)

PACS number(s): 03.75.Hh, 05.30.Jp, 03.75.Kk, 03.75.Mn

I. INTRODUCTION

The behavior of macroscopic systems of multicomponent bosons under suitable constraints can often be greatly simplified through a quantum rotor description. Within the context of condensed matter physics, the most widely appreciated example is the celebrated Josephson model [1,2]. This model provides an accurate low-energy treatment of two superconductors linked by an insulating barrier [3]. The treatment of the full many-particle system reduces to a model with two canonically conjugate variables: the relative particle number and the phase between the two superconducting regions.

Bose-Einstein condensates composed of atoms with internal spin or pseudospin degrees of freedom, the so-called spinor condensates, offer another arena where such rotor mappings are highly useful. Roughly speaking, recent experimental work investigating the dynamics of spinor condensates can be divided into two categories. The first category of experiments focuses on the complex interplay between spatial and spin degrees of freedom resulting from spinor condensates in larger traps [4–9]. These experiments investigate the dynamics after a quantum quench, which involves the proliferation of topological defects. The second category of experiments is performed in tight traps where the spatial degrees of freedom are unimportant [10–18]. Such experiments have focused on the coherent spin dynamics after preparing the system in a particular manner. The rotor description is useful when the spatial degrees of the condensate can be neglected and thus is particularly relevant to the second class of experiments.

In an early theoretical work on spinor condensates it was shown that the ground state of the antiferromagnetic condensate in tight traps involves large spin correlations and can be considered to be a condensate of singlet pairs of spin-one atoms [19]. However, such “fragmented” states [20,21] are known to be extremely delicate and for most experimental situations are typically better described by a broken-symmetry state, which is captured by the classical Gross-Pitaevskii theory [22–24]. Nevertheless the intriguing

properties of the fragmented condensates in the single-mode regime have motivated a considerable amount of further theoretical work [25–30].

In this paper we will revisit this problem by employing an exact rotor mapping. The mapping, which was carried out by some of us in a previous work [31], maps an antiferromagnetic spin-one condensate in an external field onto a quantum rotor model of a particle under an external field constrained to the unit sphere [31]. Since this mapping is exact, and not a low-energy theory, it treats all possible phases of the spin-one condensate on an equal footing. Roughly speaking, states described by the Gross-Pitaevskii equation (GPE) correspond to rotor states that are well localized in position. On the other hand, states that are delocalized over the sphere (e.g., the condensate of singlet pairs of atoms) cannot be described by the GPE but are contained within this rotor treatment. We will provide in-depth analysis of the model and discuss its distinct physical regimes. We will also describe its semiclassical limit, which has a clearer physical interpretation than the GPE, and elucidate the semiclassical behavior of the rotor wave functions for appropriate parameter regimes. We will also describe how to extend the mapping to systems with larger spin. In that sense, the current work is a generalization and extension of Ref. [31].

The paper is organized as follows. In Sec. II, for completeness, we consider the simplest nontrivial example of bosons in a double-well potential and map this system onto a quantum rotor model. We arrive at a result first obtained in Ref. [32], but we use a method that can be generalized to systems with more components, i.e., higher spins. In Sec. III we move on to the more complex case of a spin-one condensate in the single-mode regime and provide an overview of the rotor mapping originally derived by some of us in Ref. [31]. In Sec. IV we consider the correspondence between the eigenvalues of the original bosonic problem (which has a finite spectrum for fixed particle number) and the rotor model (which has an unbounded spectrum from above). In Sec. V

we consider in more detail the spectrum of the rotor model and establish three distinct physical limiting cases, namely, the Rabi, Josephson, and Fock regimes. We provide analytic expressions for the low-lying spectrum for these cases. In Sec. VI we consider the semiclassical limit of the rotor model. Here we discuss recent experiments on ^{23}Na dynamics in terms of the semiclassical phase space. We then connect the quantum mechanical wave functions in the Rabi and Josephson regimes to the semiclassical phase space using a generalization of the Husimi distribution function [33,34]. In Sec. VII we consider extending the rotor mapping to larger component systems, focusing on the example of the spin-two condensates. Finally, in Sec. VIII we conclude with a summary.

II. BOSONS IN A DOUBLE-WELL POTENTIAL

In this section, we consider the simplest nontrivial case of bosons in a double-well potential that is described by the two-site Bose-Hubbard model. This archetypal model has been studied extensively [21,32,35–37] and has also been used to experimentally observe the so-called self-trapping effect [38]. In the interesting work of Anglin *et al.* [32] it was shown that the two-site Bose-Hubbard model can be exactly mapped onto a two-dimensional quantum rotor model. Below we will derive their main result, using a different formalism that allows a more direct generalization to higher-dimensional rotor systems, which will be considered in following sections. We clarify our notations and lay out the main theoretical framework in this section by considering the double-well case first.

Our starting point is the two-site Bose-Hubbard model, which describes bosons in a double-well potential with repulsive interactions:

$$H = -J(a_1^\dagger a_2 + a_2^\dagger a_1) + \frac{1}{2}Un_1(n_1 - 1) + \frac{1}{2}Un_2(n_2 - 1). \quad (1)$$

Here a_1^\dagger and a_2^\dagger create bosons in the left and right wells, respectively, $n_\alpha = a_\alpha^\dagger a_\alpha$ is the particle number operator, J is the hopping, and U is the on-site repulsion. It is often instructive to use the amplitude-phase representation of the bosonic operators. That is, we can write $a = \sqrt{n_\alpha}e^{i\theta_\alpha}$ and impose the commutation relation $[n_\alpha, \theta_\beta] = i\delta_{\alpha\beta}$. Inserting these relations into Eq. (1) and expanding to leading order in the total particle number $N = n_1 + n_2$ (which is taken to be fixed) lead to the well-known Josephson model [1,2]:

$$H_{\text{Jos}} = -JN \cos(\theta) + Un^2, \quad (2)$$

where $\theta = \theta_1 - \theta_2$ and $n = (n_1 + n_2)/2$ so that the two operators in this equation are canonically conjugate: $[n, \theta] = i$. The spectrum of the Josephson model can be seen to agree with the original double-well model Eq. (1) in the large-particle number limit.

In the work of Anglin *et al.* [32], it was shown that such a mapping can be made exact and thus will reproduce the spectrum of Eq. (1) for arbitrary particle numbers. Their derivation used a method akin to the Bargmann phase-space representation of bosonic operators [39]. Here we will derive

their central result through a different method. To start, we define the states

$$|\Omega_N\rangle = \frac{1}{\sqrt{2^N N!}}(a_1^\dagger e^{i\theta} + a_2^\dagger e^{-i\theta})^N |0\rangle \quad (3)$$

$$= \frac{1}{\sqrt{N!}}(\mathbf{\Omega} \cdot \mathbf{b}^\dagger)^N |0\rangle, \quad (4)$$

where $\mathbf{\Omega} = (\cos(\theta), \sin(\theta))$ is a real two-component vector on the unit circle and the ‘‘Cartesian’’ bosonic operators b_x and b_y are defined to be $b_x = \frac{1}{\sqrt{2}}(a_1 + a_2)$, $b_y = \frac{i}{\sqrt{2}}(a_1 - a_2)$. These states can be shown to form an overcomplete basis. For instance, the fragmented state $(a_1^\dagger)^{N/2}(a_2^\dagger)^{N/2}|0\rangle$ can be seen to be an equal-weight superposition of these states over the unit circle [21]. Therefore, an arbitrary state $|\Psi\rangle$ in the bosonic Hilbert space can be expressed in terms of a superposition over the states $|\Omega_N\rangle$ with weight factor $\psi(\mathbf{\Omega})$:

$$|\Psi\rangle = \int d\Omega |\Omega_N\rangle \psi(\mathbf{\Omega}). \quad (5)$$

Note that due to the overcompleteness, this relation does not uniquely determine $\psi(\mathbf{\Omega})$. The approach of the mapping is to find a Hamiltonian \mathcal{H} acting in the ‘‘rotor’’ space such that

$$\int d\Omega (H|\Omega_N\rangle)\psi(\mathbf{\Omega}) = \int d\Omega |\Omega_N\rangle [\mathcal{H}\psi(\mathbf{\Omega})]. \quad (6)$$

Then the rotor Schrödinger equation $\mathcal{H}\psi = i\partial_t\psi$ is a sufficient condition for the bosonic Schrödinger equation to be satisfied (we will work in units where $\hbar = 1$ unless otherwise stated).

In obtaining \mathcal{H} , we use the gradient operator ∇ on the unit circle, which in terms of θ is $\nabla_x = -\sin(\theta)\partial_\theta$ and $\nabla_y = \cos(\theta)\partial_\theta$. These derivatives satisfy the geometrically intuitive relations

$$\nabla_\alpha \Omega_\beta = \delta_{\alpha\beta} - \Omega_\alpha \Omega_\beta. \quad (7)$$

(For a discussion, see Appendix A.) With this, it can be seen that quadratic operators acting on $|\Omega_N\rangle$ can be written as

$$b_\alpha^\dagger b_\beta |\Omega_N\rangle = \Omega_\beta (\nabla_\alpha + N\Omega_\alpha) |\Omega_N\rangle. \quad (8)$$

In terms of the Cartesian operators, the double-well Hamiltonian (up to a constant offset) is

$$H = -J(b_x^\dagger b_x - b_y^\dagger b_y) + \frac{U}{4}(ib_x^\dagger b_y - ib_y^\dagger b_x)^2. \quad (9)$$

We can now use the relation in Eq. (8) to find

$$(b_x^\dagger b_x - b_y^\dagger b_y) |\Omega_N\rangle = (N \cos(2\theta) - \sin(2\theta)\partial_\theta) |\Omega_N\rangle \quad (10)$$

and

$$(ib_x^\dagger b_y - ib_y^\dagger b_x)^2 |\Omega_N\rangle = L_{xy}^2 |\Omega_N\rangle, \quad (11)$$

where $L_{xy} = -i\Omega_x \nabla_y + i\Omega_y \nabla_x = -i\partial_\theta$. The effective rotor Hamiltonian can then be obtained by inserting these relations into Eq. (6) and integrating by parts. One finds

$$\mathcal{H} = \frac{1}{4}Un^2 - J(N+2)\cos(2\theta) - iJ\sin(2\theta)n, \quad (12)$$

where $n = i\partial_\theta$. While the operator \mathcal{H} has a real spectrum, it is not Hermitian due to its last term. However, one can apply

a similarity transform to render \mathcal{H} Hermitian. Specifically, defining [32]

$$\mathcal{H} = e^{\cos(2\theta)\frac{J}{U}} \mathcal{H} e^{-\cos(2\theta)\frac{J}{U}} \quad (13)$$

and shifting $\theta \rightarrow \theta/2$ to compare with Eq. (2), one finds

$$\mathcal{H} = Un^2 - J(N+1)\cos(\theta) + \frac{J^2}{U}\sin^2(\theta), \quad (14)$$

which is the main result. This model can be interpreted as a quantum-mechanical particle with momentum n moving on the unit circle under the potential $V(\theta) = -J(N+1)\cos(\theta) + \frac{J^2}{U}\sin^2(\theta)$. When N is large, the first term in the potential is dominant, and the model reduces to the familiar Josephson model equation (2). The additional terms in Eq. (2), however, serve to make the spectrum of the original double-well Hamiltonian equation (1) exactly match the eigenstates of this rotor model.

III. SPIN-ONE CONDENSATES IN THE SINGLE-MODE REGIME

We now move on to discuss the related, but more complex, problem of the spinor condensate in the single-mode regime under a magnetic field. Recently, it was shown [31] that this system maps onto a quantum rotor model under an external magnetic field. Here we will summarize this mapping.

Our starting point is a spin-one condensate in a trap that is sufficiently tight such that it is a good approximation to take all of the bosons to occupy the same spatial mode. Under this approximation, we can write the field operators for each spin state as

$$\psi_\alpha(\mathbf{r}) = \phi(\mathbf{r})a_\alpha, \quad (15)$$

where α runs from -1 to 1 . The condensate profile satisfies

$$\int d^3r |\phi(\mathbf{r})|^2 = N, \quad (16)$$

where N is the number of particles in the system. This approximation, commonly referred to as the single-mode approximation, breaks down when the condensate spin coherence length is smaller than the condensate size.

The Hamiltonian for this system reads

$$H = \frac{g}{2N} F^2 - qa_0^\dagger a_0. \quad (17)$$

In this equation, $\mathbf{F} = a_\alpha^\dagger \mathbf{F}_{\alpha\beta} a_\beta$ is the total spin operator, where $\mathbf{F}_{\alpha\beta}$ are spin-one matrices, g is the spin-dependent interaction, and q is the quadratic Zeeman shift due to an external magnetic field. Note that there is typically also a linear Zeeman term proportional to F_z for spinor condensates. Such a term commutes with H in Eq. (17) and therefore can be removed by a simple unitary transformation. However, when away from the single-mode regime, spatial dependence of the linear Zeeman will have nontrivial consequences on the dynamics. Taking a uniform condensate density $\phi(\mathbf{r}) = \sqrt{n_0}$, we can express g in terms of microscopic parameters as

$$g = \frac{4\pi\hbar^2}{3m} (\bar{a}_2 - \bar{a}_0)n_0, \quad (18)$$

where m is the mass of the constituent atoms and \bar{a}_0 and \bar{a}_2 are the scattering lengths. We will focus on the case of antiferromagnetic interactions for which $g > 0$, as is the case for ^{23}Na condensates.

As was done for the double-well problem in Sec. II, it is useful to transform the bosonic operators to the Cartesian basis, rewriting the operators as $b_x = -(a_1 - a_{-1})/\sqrt{2}$, $b_y = (a_1 + a_{-1})/i\sqrt{2}$, and $b_z = a_0$. Written in terms of these, the spin operator becomes $\mathbf{F} = -i\mathbf{b}^\dagger \times \mathbf{b}$. We next define the overcomplete set of states as

$$|\mathbf{\Omega}_N\rangle = \frac{1}{\sqrt{N!}} (\mathbf{\Omega} \cdot \mathbf{b}^\dagger)^N |0\rangle, \quad (19)$$

which are parametrized by a three-component vector on the unit sphere $\mathbf{\Omega}$ (note that the analogous states in Sec. II were parameterized on the unit circle).

The general mapping proceeds with the general method given above in Sec. II. Namely, one writes a general bosonic wave function as a superposition of states in the $|\mathbf{\Omega}_N\rangle$ basis and finds an operator \mathcal{H} acting in the rotor Hilbert space that satisfies Eq. (6) (where the integration is generalized to the unit sphere). The full derivation is given in Ref. [31], and thus, we will only give the results here. The rotor Hamiltonian corresponding to Eq. (17) is

$$\mathcal{H} = \frac{g}{2N} L^2 - q(N+3)\Omega_z^2 + q\Omega_z \nabla_z, \quad (20)$$

where L_α is the angular momentum operator and ∇_α are the gradient operators on the unit sphere. In the spherical coordinate representation, $\nabla_z = -\sin(\theta)\partial_\theta$. This can be brought to the more intuitive Hermitian form by applying a similarity transformation. In particular, defining $\mathcal{H} = e^{-S} \mathcal{H} e^S$, where $S = \frac{qN}{4g} \cos(2\theta)$, we find

$$\mathcal{H} = \frac{1}{2I} L^2 + V(\theta), \quad (21)$$

where $I = N/g$ is the moment of inertia and

$$V(\theta) = q \left(N + \frac{3}{2} \right) \sin^2(\theta) + \frac{q^2 N}{8g} \sin^2(2\theta) \quad (22)$$

is the external potential. The spectrum of this Hamiltonian exactly matches that of Eq. (17). As was described in [31], one must retain only the eigenstates of this rotor model that are symmetric under inversion: $\psi(\mathbf{\Omega}) = \psi(-\mathbf{\Omega})$. However, since the operator that projects into this subspace of states commutes with the rotor Hamiltonian, this imposes no additional conceptual or technical difficulty.

Since ϕ does not appear in the potential V in Eq. (21), one notes that this rotor model has azimuthal symmetry. This symmetry essentially reduces the model to a one-dimensional system that considerably simplifies computations. For this case, one can set $L^2 = -\frac{1}{\sin^2\theta} \partial_\theta (\sin\theta \partial_\theta) - \frac{m^2}{\sin^2\theta}$, where m is the azimuthal quantum number, and solve this one-dimensional Schrodinger equation. One should note, however, that we did not rely on this symmetry in the derivation, and it will not be present for more general couplings. In Appendix B we provide a rotor mapping for a more general coupling.

IV. CORRESPONDENCE OF THE ROTOR AND BOSONIC EIGENVALUES

There are subtleties that arise due to the fact that the rotor model equation (21) has an unbounded spectrum from above, while the spectrum of the original bosonic problem for fixed particle number N is finite. As is clear from the mapping, an eigenstate of the rotor model ψ is a sufficient condition for an eigenstate of the bosonic Hamiltonian $|\Psi\rangle$. That is, given ψ , one can construct the bosonic eigenstate through

$$|\Psi\rangle = \int d\Omega |\Omega_N\rangle \psi(\Omega). \quad (23)$$

Here for simplicity we are taking ψ to be an eigenstate of the non-Hermitian rotor model \mathcal{H} so that we do not need to include factors of e^S . Because the spectrum of the bosonic Hamiltonian H is bounded, the only possibility is that many of the rotor eigenstates get transformed to $|\Psi\rangle = 0$ through Eq. (23), noting that this trivially satisfies the bosonic Schrödinger equation. Following Ref. [32], we will refer to the rotor eigenstates that transform to $|\Psi\rangle \neq 0$ as “physical” and those that transform to $|\Psi\rangle = 0$ as “unphysical.”

We next ask if all of the eigenstates of the bosonic spectrum are included in the rotor description. For instance, the pathological case of all the rotor eigenstates mapping to $|\Psi\rangle = 0$ is not *a priori* ruled out. Another question that arises regards the ordering of the unphysical and physical eigenstates. In particular, is there an energy cutoff below which all eigenstates are physical and above which eigenstates are unphysical? We will show that there is an affirmative answer to both of these questions.

For sufficiently small particle number N , the eigenspectrum of the bosonic Hamiltonian equation (17) can be numerically computed and compared to the eigenspectrum of the rotor system equation (21). The rotor Hamiltonian has azimuthal symmetry since the potential V appearing in Eq. (22) does not depend on the angle ϕ . Therefore, \mathcal{H} commutes with L_z , and the eigenspectrum for fixed values $L_z = m$ can be considered separately. Similarly, F_z commutes with the bosonic Hamiltonian H , and we can compare to the rotor model by fixing $F_z = -m$. In Fig. 1 the eigenspectrums of both the rotor model and the bosonic model are shown as a function of the quadratic Zeeman field q . We take the case of relatively small particle number $N = 20$ and take fixed $F_z = L_z = 0$. As can be seen, all of the eigenenergies of the bosonic Hamiltonian are accounted for by the rotor model. Furthermore, the physical states of the rotor model are always lower in energy than the unphysical states. Similar behavior was found for other values of fixed $L_z = m \neq 0$, which are not shown.

This behavior can be understood as follows. For unphysical states $\psi(\Omega)$, it can be seen from Eq. (23) that $\langle Y_{\ell m} | \psi \rangle = 0$ for all $\ell \leq N$. It can be verified that the (non-Hermitian) rotor Hamiltonian defined in Eq. (20) has the property

$$\langle Y_{\ell m} | \mathcal{H} | Y_{\ell' m'} \rangle = 0 \quad (24)$$

for $\ell \leq N$ and $\ell' > N$. Suppose that we have a rotor eigenstate that is unphysical for parameters (q, g) . Then the eigenstate at $(q + \Delta q, g)$ can be determined by first-order perturbation theory. By doing so, one sees from Eq. (24) that if a state is

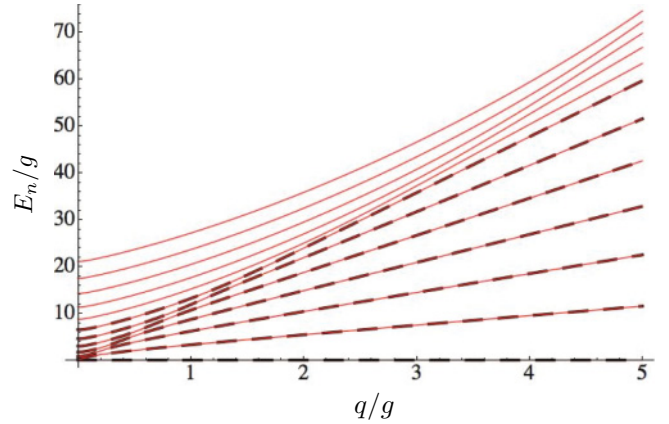


FIG. 1. (Color online) Black dashed lines: the eigenvalues E_n of the spinor bosonic Hamiltonian equation (17) for $N = 12$ particles for fixed $F_z = 0$ as a function of quadratic Zeeman field q . Red solid lines: the lowest 12 eigenvalues of the rotor Hamiltonian equation (21) for fixed $L_z = 0$ after the antisymmetric states for which $\psi(\Omega) = -\psi(\Omega)$ are projected out. The lowest (physical) eigenvalues of the rotor model exactly agree with those of the bosonic Hamiltonian. For all points in the plot, the spectrum is shifted so that the lowest eigenvalue has zero energy.

unphysical at q , then the same state will also be unphysical at $q + \Delta q$. In the limit of $q = 0$, the rotor model becomes trivial. Here the eigenstates are simply spherical harmonics with eigenenergies $E_\ell = \frac{g}{2N} \ell(\ell + 1)$. Furthermore, the lowest eigenstates for $\ell \leq N$ are all physical, while the higher eigenstates for $\ell > N$ are unphysical in this limit. We note that for fixed $L_z = m$, the rotor Hamiltonian becomes one-dimensional. Thus, there will not be any band crossings [40]. From the perturbative argument above, we therefore conclude that the higher-energy states will always remain unphysical and will not mix with the lower-energy physical states.

V. EIGENSPECTRA OF THE ROTOR MODEL

In this section we will concentrate on the eigenspectrum of the spin-one rotor Hamiltonian given in Eq. (21). We will give the spectrum in particular limiting cases and compare the results with those of the two-site Bose-Hubbard problem.

We consider how the spectrum evolves as a function of q . For large q , the potential energy $V(\theta)$ in Eq. (22) serves to localize the wave function on the unit sphere. To obtain the energy levels, the angular momentum L^2 can be expanded about the north pole so that \mathcal{H} becomes a two-dimensional harmonic oscillator. When $1 \ll q/g$, the second term in the potential energy $V(\theta)$ dominates so that the energy levels are given by

$$E_{(n_x, n_y)} = q(n_x + n_y), \quad (25)$$

where n_x and n_y are integers corresponding to the oscillator modes in the x and y directions. These eigenstates can, in fact, be directly obtained from the original bosonic Hamiltonian equation (17) in the large- q limit.

Next, we consider the case of smaller q where $1/N^2 \ll q/g \ll 1$. For this case, the first term in the potential energy is the most significant. Here we can also expand the kinetic

energy about the north pole to obtain a harmonic oscillator Hamiltonian. For this the energy levels read

$$E_{(n_x, n_y)} = \sqrt{2gq}(n_x + n_y), \quad (26)$$

where, as in Eq. (25), n_x and n_y are integers. As shown in Appendix C, it can be seen that the Bogoliubov spectrum of Eq. (17) agrees with Eqs. (25), (26).

Finally, we consider the case of vanishingly small magnetic field such that $q/g \ll \frac{1}{N^2}$. For this case the eigenfunctions are not localized about the north pole. The kinetic energy $\frac{1}{2I}L^2$ dominates the rotor model, and the eigenstates are given simply by

$$E_\ell = \frac{g}{2N}\ell(\ell + 1). \quad (27)$$

Each of these energy levels has multiplicity $2\ell + 1$. So that the wave function has inversion symmetry, only even values of ℓ should be kept. The ground state in this regime where the rotor is completely delocalized about the unit sphere, in terms of the bosonic model, is the fragmented condensate composed of singlet pairs of bosons. However, due to the condition $q/g \ll 1/N^2$, in the thermodynamic limit any small magnetic field will drive the system to a symmetry-broken state, which is described well by mean-field theory [22–24]. This is the central difficulty in experimentally realizing the singlet condensate. We will address this problem in more detail in Appendix D.

It is instructive to compare the above results with the two-site Bose-Hubbard model. This model has been analyzed and found to have three distinct limits, namely, the Rabi, Josephson, and Fock regimes, using the terminology of Leggett [37,41]. Using a method very similar to that used above, the expressions for the energy eigenstates can be obtained in these regimes from the rotor Hamiltonian in Eq. (14). Namely, for the Rabi regime where $N \ll J/U$ the last term in the potential energy dominates, and the spectrum is approximated by a harmonic oscillator, after expanding about $\theta = 0$. The Josephson regime occurs when the first term in the potential energy dominates $1/N \ll J/U \ll N$. Here the states are also localized about $\theta = 0$. Finally, for $J/U \ll 1/N$ the Fock regime is obtained where the rotor is delocalized over the unit circle. The Josephson Hamiltonian equation (2) correctly describes the Fock and Josephson regimes but cannot describe the Rabi regime since a large- N expansion is used to derive it. In summary, the three possible regimes for the two-site Bose-Hubbard model are

$$N \ll J/U, \quad (28)$$

$$1/N \ll J/U \ll N, \quad (29)$$

$$J/U \ll 1/N, \quad (30)$$

for the Rabi, Josephson, and Fock regimes, respectively.

It is clear that there is a close parallel between the above-described regimes for the two-site Bose-Hubbard model and those of the spin-one condensate problem. For this reason we will adopt the terminology introduced in [37,41] for the spinor problem. Namely, we will label the three regimes as [42]

$$1 \ll q/g, \quad (31)$$

$$1/N^2 \ll q/g \ll 1, \quad (32)$$

$$q/g \ll 1/N^2, \quad (33)$$

for the Rabi, Josephson, and Fock regimes, respectively. For typical experimental situations (for example, those described in Refs. [17,18]) $q \sim g$ and $N \sim 10^3 - 10^5$, which places the system in either the Rabi or Josephson regimes. For these cases, the Gross-Pitaevskii equation gives a qualitatively correct description of the dynamics. It is also interesting to note that for double-well condensates the Rabi regime is more difficult to achieve since by reducing the hopping J to achieve the condition in Eq. (28), a single-band description becomes inapplicable. On the other hand, the Fock regime for double-well condensates can be experimentally achieved, which has the Mott insulating ground state [43,44].

VI. SEMICLASSICAL ANALYSIS OF THE ROTOR MODEL

In this section we analyze the semiclassical limit of the rotor model in Eq. (21). We will use this to address recent experimental results. We will then show results from taking the Husimi transform of the quantum eigenstates of the rotor model. Such a method has been shown to elucidate the semiclassical limit of the two-site Bose-Hubbard model [34].

In recent experiments [17,18] the dynamics of a ^{23}Na condensate, which has antiferromagnetic interactions $g > 0$, was investigated. The initial condensate was prepared in a fully polarized ferromagnetic state pointing in the x direction after which the condensate was allowed to freely evolve. The value of $\langle F_x \rangle^2$ was measured as a function of time. Two distinct types of behavior were found, depending on the external magnetic field, which couples to the system through the quadratic Zeeman shift q . A separatrix between these two behaviors occurs at a critical magnetic field B_c . When $B < B_c$, $\langle F_x \rangle^2$ showed oscillatory behavior, having $\langle F_x \rangle^2 > 0$ at all times. On the other hand, when $B > B_c$, it was seen that $\langle F_x \rangle^2 = 0$ at periodic intervals during its evolution. An analysis of the behavior was provided in terms of the classical Gross-Pitaevskii energy functional. Taking into account the conserved quantities (total particle number and spin moment in the z direction, which was fixed to be $\langle F_z \rangle = 0$), the two-dimensional phase portrait of the energy functional was shown to capture these two regimes.

We will now describe how the semiclassical limit of Eq. (21) gives an intuitive understanding of these results. The corresponding Lagrangian is

$$\mathcal{L} = \frac{1}{2}I[\dot{\theta}^2 + \sin^2(\theta)\dot{\phi}^2] - V(\theta), \quad (34)$$

where $V(\theta)$ is given by Eq. (22). This gives the canonical momenta $p_\theta = I\dot{\theta}$ and $p_\phi = I\sin^2(\theta)\dot{\phi}$. The corresponding classical energy is

$$E = \frac{1}{2I}\left(p_\theta^2 + \frac{p_\phi^2}{\sin^2(\theta)}\right) + V(\theta). \quad (35)$$

The above equations describe the motion of a particle on a unit sphere. We will concentrate on the case where $p_\phi = 0$. The classical equal-energy contours of Eq. (35) are plotted in Fig. 2(a). Two types of behavior are seen. The higher-energy states have motion where the particle's trajectory explores both hemispheres but has either $p_\theta > 0$ or $p_\theta < 0$ at all times, thus never having zero angular momentum. This corresponds to the motion of the spin-one condensate for $B < B_c$. Increasing the magnetic field will constrain the particle's trajectory to

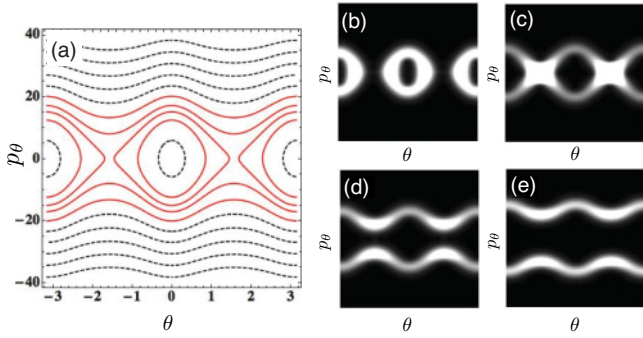


FIG. 2. (Color online) (a) Equal-energy contours of the semiclassical energy given in Eq. (35) for $p_\phi = 0$. (b–e) Husimi distribution functions $H(\mathbf{z})$ for particular eigenstates of the rotor model Eq. (21) for the parameters $q = g$, $N = 10$, and $\kappa = 1/10$. Panels (b), (c), (d), and (e) respectively correspond to the second, fourth, sixth, and eighth excited states within the manifold of $m = 0$ and even ℓ . The classical equal-energy contours corresponding to these energies are plotted with solid red lines (otherwise, the contours are plotted with black dashed lines). The same range of p_θ and θ is used for all plots.

one hemisphere. For this motion, it is seen that $p_\theta = 0$ at periodic intervals during the particle's trajectory. This type of motion corresponds to $B > B_c$ of the spin-one condensate experiment [45].

We will now move on to discuss the semiclassical properties manifest in the quantum mechanical wave functions of Eq. (21) for appropriate parameter regimes. To do this, we will use a generalization of the Husimi distribution function [33] to the case of the sphere. The Husimi distribution function has been successfully applied to elucidate the pendulum structure manifest in the wave functions of double-well condensates [34] described by Eq. (1).

Conventionally, the Husimi distribution function of a particular wave function $|\psi\rangle$ is defined as

$$H(\mathbf{z}) = \frac{|\langle \mathbf{z} | \psi \rangle|^2}{\langle \mathbf{z} | \mathbf{z} \rangle}, \quad (36)$$

where $|\mathbf{z}\rangle$ is a scaled coherent state. For our considerations, we thus need a generalization of the notion of a coherent state to the unit sphere. Recent work on such a generalization is given in Refs. [46,47]. In [46] it was argued that it is most natural to define spherical coherent states to be eigenstates of the ‘‘annihilation’’ operators

$$A_\alpha = e^{-\frac{1}{2}\kappa L^2} \Omega_\alpha e^{\frac{1}{2}\kappa L^2}, \quad (37)$$

where κ is a scaling parameter [48]. Such eigenstates are given by

$$|\mathbf{z}\rangle = \sum_{\ell m} e^{-\kappa \ell(\ell+1)/2} |Y_{\ell m}\rangle Y_{\ell m}^*(\mathbf{z}). \quad (38)$$

In this equation \mathbf{z} is a three-component complex vector that satisfies $\mathbf{z} \cdot \mathbf{z} = 1$. In terms of classical phase-space variables ($\mathbf{p} = p_\theta \hat{\theta} + p_\phi \hat{\phi}$ and Ω), \mathbf{z} can be expressed as [46]

$$\mathbf{z} = \cosh(\kappa p) \Omega + i \frac{1}{p} \sinh(\kappa p) \mathbf{p}. \quad (39)$$

The value of the scaling parameter should be taken such that $\kappa^2 \sim \frac{g}{qN^2}$, which is the ratio of the prefactors of the kinetic and potential energies in Eq. (21).

We consider the case where $q = g$ and $N = 10$ bosons, which places the system between the Josephson and Rabi regimes and well away from the Fock regime. Density plots of the Husimi distribution function for particular rotor eigenstates are shown in Figs. 2(b)–2(e). Since we concentrate on the case of $F_z = 0$, the Husimi distribution function will only depend on the pair of variables (θ, p_θ) . Red classical equal-energy contours shown in Fig. 2(a) are drawn for energies corresponding to these eigenstates. One sees that the Husimi distribution functions strongly resemble the semiclassical contours, thus revealing the semiclassical behavior of the eigenstates. Such agreement occurs for all states in the Rabi and Josephson regimes but not for the Fock regime, which has no semiclassical correspondence.

VII. EXTENSION TO HIGHER SPINS

We will now move on to discuss how to perform the rotor mapping for larger-spin systems. We will focus on $F = 2$ spinor condensates because of their experimental availability as hyperfine states of alkali atoms. We will show that this system maps to a particle moving on a sphere in five-dimensional space.

Spin-two condensates have five spin components. We take a_α for $\alpha = -2, \dots, 2$ to annihilate a boson with $F_z = \alpha$. In the single-mode regime, spin-two condensates are described by the Hamiltonian [49]

$$H = \frac{g_1}{2N} F^2 + \frac{g_2}{2N} \mathcal{A}^\dagger \mathcal{A}. \quad (40)$$

Here $\mathbf{F} = a_\alpha^\dagger \mathbf{F}_{\alpha\beta} a_\beta$ is the total spin operator, where $\mathbf{F}_{\alpha\beta}$ are spin-two matrices. In the second term, $\mathcal{A} = a_0 a_0 - 2a_1 a_{-1} + 2a_1 a_{-1}$ annihilates a singlet pair of bosons. In terms of physical quantities, the coefficients $g_{1,2}$ are given by

$$g_1 = \frac{4\pi\hbar^2}{7m} n_0 (\bar{a}_4 - \bar{a}_2), \quad (41)$$

$$g_2 = \frac{4\pi\hbar^2}{m} n_0 \left(\frac{1}{5} (\bar{a}_0 - \bar{a}_4) - \frac{2}{7} (\bar{a}_2 - \bar{a}_4) \right), \quad (42)$$

where \bar{a}_0 , \bar{a}_2 , and \bar{a}_4 are the spin-two s -wave scattering lengths. For simplicity, we will neglect the effects of an external magnetic field on this system.

We perform the following unitary transformation on the bosonic operators:

$$b_1 = a_0, \quad (43)$$

$$b_2 = \frac{1}{i\sqrt{2}} (-a_{-1} - a_1), \quad (44)$$

$$b_3 = \frac{1}{\sqrt{2}} (a_{-1} - a_1), \quad (45)$$

$$b_4 = \frac{1}{i\sqrt{2}} (a_2 - a_{-2}), \quad (46)$$

$$b_5 = \frac{1}{\sqrt{2}} (a_2 + a_{-2}). \quad (47)$$

These operators transform as a vector under SO(5) rotations generated by $M_{\alpha\beta} = -i(b_\alpha^\dagger b_\beta - b_\beta^\dagger b_\alpha)$. In terms of these quantities, the singlet operator is

$$\mathcal{A} = \mathbf{b} \cdot \mathbf{b}, \quad (48)$$

while the spin operators are

$$F_x = \sqrt{3}M_{12} - M_{25} + M_{34}, \quad (49)$$

$$F_y = \sqrt{3}M_{13} + M_{24} + M_{35}, \quad (50)$$

$$F_z = M_{23} + 2M_{45}. \quad (51)$$

As before, we can parametrize an overcomplete set of states (but now using the five-component, real unit vector Ω) as

$$|\Omega_N\rangle = \frac{1}{\sqrt{N!}} \left(\sum_{\alpha=1}^5 \Omega_\alpha b_\alpha^\dagger \right) |0\rangle. \quad (52)$$

The mapping proceeds along similar lines to that in Secs. II and III. In particular, one finds that

$$M_{\alpha\beta} \rightarrow -L_{\alpha\beta}, \quad (53)$$

where $L_{\alpha\beta} = -i(\Omega_\alpha \nabla_\beta - \Omega_\beta \nabla_\alpha)$. This can be used to find the rotor correspondence of the first term in Eq. (40).

Next, we find the rotor correspondence of the second term in Eq. (40). We use the five-component version of Eq. (8) to find that

$$\mathcal{A}^\dagger \mathcal{A} |\Omega_N\rangle = (\nabla^2 + N^2 + 3N) |\Omega_N\rangle. \quad (54)$$

In this equation, ∇^2 is the Laplacian on the five-dimensional hypersphere, as described in Appendix A. The integration by parts here is straightforward. One obtains

$$\mathcal{A}^\dagger \mathcal{A} \rightarrow \nabla^2 + N^2 + 3N. \quad (55)$$

The resulting rotor model, which is already Hermitian, is thus

$$\begin{aligned} \mathcal{H} = & \frac{g_2}{2N} \nabla^2 + \frac{g_1}{2N} [(\sqrt{3}L_{12} - L_{25} + L_{34})^2 \\ & + (\sqrt{3}L_{13} + L_{24} + L_{35})^2 + (L_{23} + 2L_{45})^2], \end{aligned} \quad (56)$$

where we have dropped a constant energy offset. This model has a particularly simple form in the limit of $g_1 = 0$. Here the system has an SO(5) symmetry, and the ground state will be a condensate of singlet pairs of spin-two bosons.

VIII. CONCLUSION

In this work we have analyzed in detail rotor mappings of spinor condensates in the single-mode regime. We have addressed some subtleties related to the physical and unphysical eigenstates and showed that the rotor mapping gives an exact treatment of the spinor condensate. Since the rotor model treats the mean field as well as correlated phases on equal footing, it offers new insights into the problem. We have established both the importance of the rotor model in providing physical insight into the properties of spinor condensates and its validity as a practical scheme for carrying out calculations.

There are several interesting directions that can be pursued in future work. The Husimi distribution function has proven useful for understanding the collapse and revival process of atoms in the proximity of a superfluid-insulating phase transition [44]. Such a phase-space analysis of the collapse

and revival dynamics for the spinor system close to the Fock regime will prove to be valuable. We emphasize that for this regime the semiclassical correspondence illustrated in Fig. 2 will not hold.

In Sec. VII we derived the rotor representation of the spin-two system for a single site. The mean-field phase diagram of the spin-two condensates is known to have a degeneracy for nematic states [50], which is lifted by quantum and thermal fluctuations [51,52]. A generalization equation (56) to include quadratic Zeeman field will prove useful for studying this effect for smaller condensates where quantum effects are more pronounced.

Future work can also investigate the rotor mapping for ferromagnetic condensates (negative g). The corresponding rotor model for this case can be interpreted as a particle with negative mass moving on the unit sphere. Finally, we note that low-energy effective rotor theories of spinor condensates (without magnetic fields) were previously investigated in [53–55]. It will be interesting to investigate how the rotor mapping generalizes to include spatial degrees of freedom.

ACKNOWLEDGMENTS

It is our pleasure to acknowledge useful discussions with A. Lamacraft, P. Lett, and W. Reinhardt. This work was supported by the NSF Joint Quantum Institute Physics Frontier Center. We are thankful for the hospitality of the Kavli Institute of Theoretical Physics under Grant No. NSF PHY05-51164, where part of this work was completed.

APPENDIX A: QUANTUM MECHANICS ON THE HYPERSPHERE

In this Appendix, for convenience, we will tabulate the properties of a particle constrained to the surface of a d -dimensional hypersphere. The position of the particle is given by d coordinates Ω_α (for $\alpha = 1, \dots, d$) subject to the constraint $\Omega \cdot \Omega = 1$. The momentum operators are $\pi_\alpha = -i\nabla_\alpha$, where ∇_α is the gradient operator in the α direction on the hypersphere (which can be expressed in terms of $d - 1$ angles and their derivatives). Finally, the angular momentum operators are $L_{\alpha\beta} = \Omega_\alpha \pi_\beta - \Omega_\beta \pi_\alpha$. Note that for $d = 3$, the angular momentum is conventionally written with a single subscript as $L_\alpha = \frac{1}{2} \varepsilon_{\alpha\beta\gamma} L_{\beta\gamma}$. The position and angular momentum are Hermitian operators, while the Hermitian conjugate of π_α is

$$\pi_\alpha^\dagger = \pi_\alpha + i(d - 1)\Omega_\alpha. \quad (A1)$$

The following commutation relations are satisfied for the position and momentum operators:

$$[\Omega_\alpha, \Omega_\beta] = 0, \quad (A2)$$

$$[\Omega_\alpha, \pi_\beta] = i(\delta_{\alpha\beta} - \Omega_\alpha \Omega_\beta), \quad (A3)$$

$$[\pi_\alpha, \pi_\beta] = -iL_{\alpha\beta}. \quad (A4)$$

These can be seen to give the angular momentum operators the correct commutation relations, which are $[L_{\alpha\beta}, L_{\gamma\delta}] = i\delta_{\alpha\gamma}L_{\beta\delta} + i\delta_{\beta\delta}L_{\alpha\gamma} - i\delta_{\alpha\delta}L_{\beta\gamma} - i\delta_{\beta\gamma}L_{\alpha\delta}$. These operators satisfy the orthogonality relation $\Omega \cdot \pi = 0$ (i.e., the

momentum and position are orthogonal on the hypersphere). It can also be verified that the total angular momentum can be expressed as

$$\frac{1}{2} \sum_{\alpha\beta} L_{\alpha\beta} L_{\beta\alpha} = \pi \cdot \pi = -\nabla^2. \quad (\text{A5})$$

APPENDIX B: ROTOR MODEL WITH GENERAL COUPLING

In this Appendix we consider spin-one Hamiltonians with more general coupling to external fields. In particular, we consider Hamiltonians of the form

$$H = \frac{g}{2N} F^2 + b_{\alpha}^{\dagger} B_{\alpha\beta} b_{\beta}, \quad (\text{B1})$$

where B is a Hermitian matrix. One can see that this reduces to Eq. (17) for the special case $B_{\alpha\beta} = -q\delta_{\alpha z}\delta_{\beta z}$. In the following, it is useful to write B in terms of its real and imaginary parts as $B = B' + iB''$. Since B is Hermitian, we have the requirement that B' is symmetric while B'' is antisymmetric.

Applying the rotor mapping as in Sec. III, one arrives at the non-Hermitian Hamiltonian

$$\mathcal{H} = \frac{g}{2N} L^2 + q(N+3)B_{\alpha\beta}\Omega_{\alpha}\Omega_{\beta} - B_{\alpha\beta}\Omega_{\beta}\nabla_{\alpha}, \quad (\text{B2})$$

which should be compared to Eq. (20). To bring this Hamiltonian to Hermitian form, we apply the similarity transformation $\mathcal{H} = e^{-S}\mathcal{H}e^S$, where

$$S = \Gamma_{\alpha\beta}\Omega_{\alpha}\Omega_{\beta}, \quad (\text{B3})$$

where Γ is a matrix. One can verify that by choosing $\Gamma = \frac{N}{2g}B'$, provided B' and B'' commute, \mathcal{H} becomes Hermitian. In particular, for this value of Γ ,

$$\mathcal{H} = \frac{1}{2I}L^2 + V(\theta, \phi), \quad (\text{B4})$$

where

$$V(\theta, \phi) = \left(N + \frac{3}{2}\right)\Omega^T B' \Omega + \frac{1}{2}B''_{\alpha\beta}L_{\beta\alpha} + \frac{N}{2g}[\Omega^T B'^2 \Omega - (\Omega^T B' \Omega)^2]. \quad (\text{B5})$$

One can check that this reduces to Eq. (21) in the appropriate limit.

APPENDIX C: THE BOGOLIUBOV SPECTRUM OF EQUATION (17)

It is instructive to compute the low-lying spectrum of the spinor Hamiltonian equation (17) through the Bogoliubov method [56] and compare with the results from the exact rotor mapping given in Sec. V. We expand about the classical mean-field state given by $\bar{a}_1 = \bar{a}_{-1} = 0$ and $\bar{a}_0 = \sqrt{N}$ and write the bosonic operators as $a_{\alpha} = \bar{a}_{\alpha} + \delta a_{\alpha}$. The constraint of fixed particle number N can be enforced up to quadratic order by requiring

$$-\sqrt{N}(\delta a_0 + \delta a_0^{\dagger}) = \delta a_1^{\dagger} \delta a_1 + \delta a_{-1}^{\dagger} \delta a_{-1}. \quad (\text{C1})$$

Dropping constant terms, Eq. (17) becomes, up to quadratic order,

$$H = (g+q)(\delta a_1^{\dagger} \delta a_1 + \delta a_{-1}^{\dagger} \delta a_{-1}) + g(\delta a_1 \delta a_{-1} + \text{H.c.}). \quad (\text{C2})$$

It is straightforward to diagonalize this by a Bogoliubov transformation. The result is

$$H = \sqrt{q(2g+q)}(\alpha^{\dagger} \alpha + \beta^{\dagger} \beta), \quad (\text{C3})$$

where α and β are bosonic annihilation operators, which is consistent with [29]. The spectrum of this Hamiltonian can be seen to agree with the results derived from the rotor model in Sec. V in the Rabi regime, Eq. (25), and Josephson regime, Eq. (26). However, the results do not agree in the Fock regime, Eq. (27), since the Bogoliubov treatment is inapplicable for a fragmented condensate.

APPENDIX D: EXPERIMENTAL REALIZATION OF THE SINGLET CONDENSATE

In this Appendix, we will discuss the experimental parameters necessary to achieve the singlet condensate. In the Josephson regime, the ground-state wave function of the rotor model is

$$\psi(\theta) = \sqrt{\frac{2}{\pi\bar{\theta}^2}} e^{-\theta^2/\bar{\theta}^2}, \quad (\text{D1})$$

where $\bar{\theta} = \sqrt{\frac{2g}{qN^2}}$. As can be verified from (32), in the Josephson regime, $\bar{\theta} \ll 1$. Decreasing the magnetic field and thereby decreasing q , one sees that the width of the wave function increases. When the width of the wave function $\bar{\theta}$ approaches unity, the harmonic description of the condensate fails, and the Fock regime is entered (33). As mentioned earlier, in the limiting case of $q = 0$ the ground state is a condensate of singlet pairs of spin-one bosons.

We thus ask what parameters are necessary for $\bar{\theta} \sim 1$. Because this quantity scales inversely with the number of particles, this state cannot be achieved in the thermodynamic limit. We therefore concentrate on systems with relatively small particle numbers. For the ^{23}Na system, the parameters g and q appearing in the rotor model equation (21) are related to the atomic density and external magnetic field B through [17]

$$g = (1.59 \times 10^{-52} \text{Jm}^3) n_0 \quad (\text{D2})$$

$$q = [1.84 \times 10^{-35} \text{J}/(\mu\text{T})^2] B^2. \quad (\text{D3})$$

For a fixed particle number, increasing the density increases $\bar{\theta}$. We thus take $n_0 = 5 \times 10^{14} \text{cm}^{-3}$, which is relatively large but still small enough that three-body losses are not important. Then, for small magnetic field $B = 0.1 \mu\text{T}$ and $N = 500$ particles, we have $\bar{\theta} = 1.9$, which is outside of the Josephson regime. If quenched from finite magnetic field, such a system will exhibit quantum collapse and revival oscillations [31].

- [1] B. D. Josephson, *Phys. Lett.* **1**, 251 (1962).
- [2] P. W. Anderson, in *Progress in Low Temperature Physics*, edited by C. J. Gorter (North-Holland, Amsterdam, 1967), Vol. 5, pp. 1–43.
- [3] M. Tinkham, *Introduction to Superconductivity* (Dover, New York, 2004).
- [4] L. E. Sadler, J. M. Higbie, S. R. Leslie, M. Vengalattore, and D. M. Stamper-Kurn, *Nature (London)* **443**, 312 (2006).
- [5] M. Vengalattore, S. R. Leslie, J. Guzman, and D. M. Stamper-Kurn, *Phys. Rev. Lett.* **100**, 170403 (2008).
- [6] C. Klempt, O. Topic, G. Gebreyesus, M. Scherer, T. Henninger, P. Hyllus, W. Ertmer, L. Santos, and J. J. Arlt, *Phys. Rev. Lett.* **103**, 195302 (2009).
- [7] M. Vengalattore, J. Guzman, S. R. Leslie, F. Serwane, and D. M. Stamper-Kurn, *Phys. Rev. A* **81**, 053612 (2010).
- [8] C. Klempt, O. Topic, G. Gebreyesus, M. Scherer, T. Henninger, P. Hyllus, W. Ertmer, L. Santos, and J. J. Arlt, *Phys. Rev. Lett.* **104**, 195303 (2010).
- [9] J. Kronjager, C. Becker, P. Soltan-Panahi, K. Bongs, and K. Sengstock, *Phys. Rev. Lett.* **105**, 090402 (2010).
- [10] J. Stenger, S. Inouye, D. M. Stamper-Kurn, H. J. Miesner, A. P. Chikkatur, and W. Ketterle, *Nature (London)* **396**, 345 (1998).
- [11] M. S. Chang, C. D. Hamley, M. D. Barrett, J. A. Sauer, K. M. Fortier, W. Zhang, L. You, and M. S. Chapman, *Phys. Rev. Lett.* **92**, 140403 (2004).
- [12] H. Schmaljohann, M. Erhard, J. Kronjager, M. Kottke, S. van Staa, L. Cacciapuoti, J. J. Arlt, K. Bongs, and K. Sengstock, *Phys. Rev. Lett.* **92**, 040402 (2004).
- [13] M. S. Chang, Q. S. Qin, W. X. Zhang, L. You, and M. S. Chapman, *Nat. Phys.* **1**, 111 (2005).
- [14] A. Widera, F. Gerbier, S. Fölling, T. Gericke, O. Mandel, and I. Bloch, *Phys. Rev. Lett.* **95**, 190405 (2005).
- [15] J. Mur-Petit, M. Guilleumas, A. Polls, A. Sanpera, M. Lewenstein, K. Bongs, and K. Sengstock, *Phys. Rev. A* **73**, 013629 (2006).
- [16] F. Gerbier, A. Widera, S. Fölling, O. Mandel, and I. Bloch, *Phys. Rev. A* **73**, 041602 (2006).
- [17] Y. Liu, S. Jung, S. E. Maxwell, L. D. Turner, E. Tiesinga, and P. D. Lett, *Phys. Rev. Lett.* **102**, 125301 (2009).
- [18] Y. Liu, E. Gomez, S. E. Maxwell, L. D. Turner, E. Tiesinga, and P. D. Lett, *Phys. Rev. Lett.* **102**, 225301 (2009).
- [19] C. K. Law, H. Pu, and N. P. Bigelow, *Phys. Rev. Lett.* **81**, 5257 (1998).
- [20] T. L. Ho and S. K. Yip, *Phys. Rev. Lett.* **84**, 4031 (2000).
- [21] E. J. Mueller, T.-L. Ho, M. Ueda, and G. Baym, *Phys. Rev. A* **74**, 033612 (2006).
- [22] T.-L. Ho, *Phys. Rev. Lett.* **81**, 742 (1998).
- [23] T. Ohmi and K. Machida, *J. Phys. Soc. Jpn.* **67**, 1822 (1998).
- [24] R. Barnett, D. Podolsky, and G. Refael, *Phys. Rev. B* **80**, 024420 (2009).
- [25] M. Koashi and M. Ueda, *Phys. Rev. Lett.* **84**, 1066 (2000).
- [26] S. Ashhab and A. J. Leggett, *Phys. Rev. A* **65**, 023604 (2002).
- [27] R. Diener and T.-L. Ho, e-print [arXiv:cond-mat/0608732](https://arxiv.org/abs/cond-mat/0608732).
- [28] L. Chang, Q. Zhai, R. Lu, and L. You, *Phys. Rev. Lett.* **99**, 080402 (2007).
- [29] X. Cui, Y. Wang, and F. Zhou, *Phys. Rev. A* **78**, 050701(R) (2008).
- [30] Q. Zhai, L. Chang, R. Lu, and L. You, *Phys. Rev. A* **79**, 043608 (2009).
- [31] R. Barnett, J. D. Sau, and S. Das Sarma, *Phys. Rev. A* **82**, 031602(R) (2010).
- [32] J. R. Anglin, P. Drummond, and A. Smerzi, *Phys. Rev. A* **64**, 063605 (2001).
- [33] K. Husimi, *Proc. Phys. Math. Soc. Jpn.* **22**, 264 (1940).
- [34] K. W. Mahmud, H. Perry, and W. P. Reinhardt, *Phys. Rev. A* **71**, 023615 (2005).
- [35] G. J. Milburn, J. Corney, E. M. Wright, and D. F. Walls, *Phys. Rev. A* **55**, 4318 (1997).
- [36] A. Smerzi, S. Fantoni, S. Giovanazzi, and S. R. Shenoy, *Phys. Rev. Lett.* **79**, 4950 (1997).
- [37] A. J. Leggett, *Rev. Modern Phys.* **73**, 307 (2001).
- [38] M. Albiez, R. Gati, J. Fölling, S. Hunsmann, M. Cristiani, and M. K. Oberthaler, *Phys. Rev. Lett.* **95**, 010402 (2005).
- [39] V. Bargmann, *Commun. Pure Appl. Math.* **14**, 187 (1961).
- [40] This can be shown by assuming two solutions to Eq. (21) with the same energy. It can be shown that the resulting Wronskian vanishes and thus the two solutions are equal to each other up to a multiplicative constant.
- [41] A. J. Leggett, in *Atomic Physics 16: 16th International Conference on Atomic Physics*, AIP Conf. Proc. No. 477, edited by W. E. Baylis and G. F. Drake (AIP, New York, 1999) p. 154.
- [42] It is also worth pointing out that the regimes $q/g \gg 1$ and $q/g \ll 1$ have been referred to as the Zeeman and mean-field regimes, respectively (see, for instance, Refs. [57, 58]).
- [43] D. Jaksch, C. Bruder, J. I. Cirac, C. W. Gardiner, and P. Zoller, *Phys. Rev. Lett.* **81**, 3108 (1998).
- [44] M. Greiner, O. Mandel, T. Esslinger, T. W. Hansch, and I. Bloch, *Nature (London)* **415**, 39 (2002).
- [45] It is also worth pointing out that experiments in double-well potentials exhibiting the self-trapping effect [38] can similarly be interpreted in terms of the classical phase space of Eq. (14). That is, this phase space also exhibits a separatrix, and trajectories with $p_\theta \neq 0$ at all times correspond to the self-trapped states.
- [46] K. Kowalski and J. Rembieliński, *J. Phys. A* **33**, 6035 (2000).
- [47] B. Hall and J. J. Mitchell, *J. Math. Phys.* **43**, 1211 (2002).
- [48] It is instructive to compare this expression to $e^{-p^2/2} x e^{p^2/2} = x + ip$ (for canonically conjugate operators x and p), which has the standard coherent states as eigenstates.
- [49] M. Ueda and M. Koashi, *Phys. Rev. A* **65**, 063602 (2002).
- [50] R. Barnett, A. Turner, and E. Demler, *Phys. Rev. Lett.* **97**, 180412 (2006).
- [51] A. M. Turner, R. Barnett, E. Demler, and A. Vishwanath, *Phys. Rev. Lett.* **98**, 190404 (2007).
- [52] J. L. Song, G. W. Semenoff, and F. Zhou, *Phys. Rev. Lett.* **98**, 160408 (2007).
- [53] F. Zhou, *Phys. Rev. Lett.* **87**, 080401 (2001).
- [54] E. Demler and F. Zhou, *Phys. Rev. Lett.* **88**, 163001 (2002).
- [55] A. Imambekov, M. Lukin, and E. Demler, *Phys. Rev. A* **68**, 063602 (2003).
- [56] N. N. Bogoliubov, *J. Phys. (USSR)* **11**, 23 (1947).
- [57] J. Kronjager, C. Becker, P. Navez, K. Bongs, and K. Sengstock, *Phys. Rev. Lett.* **97**, 110404 (2006).
- [58] J. Mur-Petit, *Phys. Rev. A* **79**, 063603 (2009).